Fuzzy Damage Mitigating Control of Mechanical Structures[1]

M. S. Holmes

Asok Ray
Fellow ASME

Mechanical Engineering Department,
The Pennsylvania State University,
University Park, PA 16802

This paper presents the architecture and synthesis of a damage mitigating control system for mechanical structures where the objective is to achieve high performance with increased reliability, availability, component durability, and maintainability. The proposed control system has a two-tier structure. In the lower tier a linear sampled-data controller tracks a reference trajectory vector while the upper tier contains a fuzzy-logic-based damage controller which makes a trade-off between system performance and the damage in critical components. The synthesis procedure is demonstrated by simulation experiments on the model of a reusable rocket engine. The simulation results explore the feasibility of automatically regulating the damage/performance trade-off in a real-time setting.

1 Introduction

A major goal in the control of complex mechanical systems such as spacecraft, advanced aircraft, and power plants is to achieve high performance with increased reliability, availability, component durability, and maintainability. The current state-of-the-art of control systems synthesis focuses on guaranteeing stability of the closed-loop system while simultaneously ensuring that the specified performance requirements are satisfied. Performance is usually defined in terms of reference signal tracking, disturbance rejection, and/or control effort minimization. However, in general, the performance specifications do not explicitly address the dynamics of material damage (e.g., fatigue cracking) in critical plant components. In view of high performance requirements and availability of improved materials, the lack of appropriate knowledge about the properties of the structural materials will lead to either less than achievable performance due to an overly conservative design, or overstraining of the critical components leading to unexpected failures and a drastic reduction in the service life of the plant. The key idea of the research work reported in this paper is that a significant improvement in service life can be achieved, especially during transient operations, by a small reduction in the dynamic performance of the system. This requires augmentation of the current system-theoretic and approximate-reasoning-based techniques for synthesis of decision and control laws with governing equations and constraints that represent the dynamic properties of the structural materials. The major challenge in this research is to characterize the damage generation process in a state-variable setting, and then utilize this information for synthesizing algorithms of robust decision and control.

Damage mitigating control is a relatively new area of research which combines the two distinct disciplines: Systems Sciences and Mechanics of Materials. Currently, there is a rather limited amount of information available on this topic in open literature. Ray et al. (1994) and Dai and Ray (1996) have shown that, in an open-loop setting, it is feasible to reduce the damage rate and accumulation in critical plant components without any significant sacrifice of the plant performance. Their damage reduction procedure, however, is based on extensive off-line optimization, and does not take advantage of on-line damage predictions or measurements for feedback control of any form. Moreover, the feedforward signal is optimized for a specific set of initial conditions and a maneuver which must be specified *a priori*. This method may not be applicable to maneuvers and/or initial conditions not used in the optimization procedure. Holmes et al. (1997) and Tangirala et al. (1997) have proposed a methodology for synthesis of robust linear control systems for damage mitigation. This approach penalizes the pertinent plant variables (e.g., turbopump torque) that directly cause damage in critical components (e.g., turbine blades), in addition to the typical performance variables such as tracking error and control effort. Although the synthesis procedure is at least implicitly based on the structural and damage model, execution of the control law does not use on-line measurements of damage and damage rate.

This paper presents a procedure for synthesizing a damage mitigating control system to achieve a desired trade-off between performance and damage via feedback of on-line measurements of damage and damage rate. The proposed control system has a two-tier structure. In the lower tier a linear sampled-data controller tracks a reference trajectory vector while the upper tier contains a fuzzy-logic-based damage controller which makes a trade-off between system performance and the damage in critical components. The synthesis procedure is demonstrated by simulation experiments on the model of a reusable rocket engine (Ray and Dai, 1995). The objective here is to explore the feasibility of automatically regulating the damage/performance trade-off in a real-time setting based on the measurements of selected process variables.

The paper is organized in six sections (including the present section) and an appendix. The architecture of the proposed damage mitigating control system is presented in Section 2. Details on the synthesis of the linear tracking controller and the damage controller are given in Sections 3 and 4, respectively. Simulation results for damage control of the rocket engine under consideration are presented in Section 5. The models of the rocket engine, turbine blade structure, and fatigue damage in the turbine blades are briefly described in Appendix A. Finally, the paper is concluded in Section 6.

2 Architecture of the Damage Mitigating Control System

The schematic diagram in Fig. 1 shows a general architecture for damage mitigating control of dynamic systems (e.g., rocket engines, aircraft, and power plants) where structural integrity is an important issue.

The plant in Fig. 1 has three types of sensor outputs: $y^{dam}(t)$, $y^{dyn}(t)$, and $y^{reg}(t)$. The vector signal $y^{dam}(t)$ contains those plant outputs that are necessary for calculation of damage (e.g.,

[1] The research work reported in this paper has been supported in part by: NASA Lewis Research Center under Grant Nos. NAG-3-1240, NAG-3-1673, NAG-3-1799 and NAG3-2016. National Science Foundation under Research Grant Nos. DMI-9424587 and CMS-9531835.

Contributed by the Dynamic Systems and Control Division for publication in the JOURNAL OF DYNAMIC SYSTEMS, MEASUREMENT, AND CONTROL. Manuscript received by the DSCD March 12, 1997. Associate Technical Editor: T. Kurfess.

Copyright © 1998 by ASME

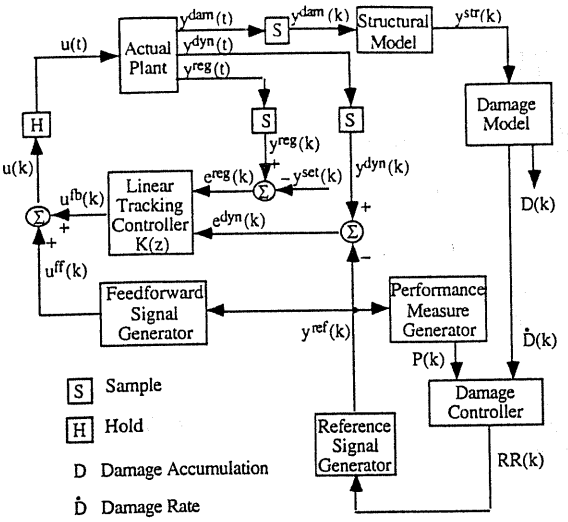

Fig. 1 Schematic diagram of damage mitigating control

torque and shaft speed for calculating turbine blade damage in a rocket engine). The vector signal $y^{dyn}(t)$ consists of the plant outputs whose reference trajectory vector is determined by the damage controller (e.g., main thrust chamber pressure in a rocket engine). The vector signal $y^{reg}(t)$ contains regulated plant outputs whose reference signals are either constants or unaltered by the damage controller. For example, the oxygen/hydrogen mixture ratio for the Space Shuttle main engine should ideally be kept at a constant value of 6.02 at all times (Ray and Dai, 1995).

The purpose of the linear tracking controller in Fig. 1 is to keep the error signals as close to zero as possible, i.e., to track $y^{set}(k)$ and $y^{ref}(k)$, and to provide robust stability in the inner control loop. Unlike the work reported by Ray et al. (1994) and Dai and Ray (1996), the feedforward control input, $u^{ff}(k)$, is not an optimized sequence. In the specific example of the control of the rocket engine, the feedforward signal generator is selected as $u^{ff}(k) = c_1 y^{ref}(k) + c_2$, where the two constants, c_1 and c_2, are identified a priori based on linear interpolation of steady state inputs.

The structural model in Fig. 1 uses the vector $y^{dam}(t)$ as an input to generate damage-causing variables such as stresses, $y^{str}(k)$. The signal $y^{str}(k)$ excites the damage model whose output is both damage rate and accumulation. The purpose of the damage model in the outer control loop is to capture the dynamic characteristics of material degradation under stress. The critical components being considered in this paper are the H_2 (fuel) turbine blades and the O_2 (oxidizer) turbine blades. (The rocket engine under consideration is briefly described in Appendix A.) The blades in these turbines are susceptible to fatigue cracks. The damage model is highly nonlinear and is normalized to have an output in the range [0, 1] where a value of 0 can be interpreted as zero damage and a value of 1 implies that the service life of the component has ended. The damage model used in the damage feedback loop provides a measure of damage rate to the Damage Controller. Since damage is not reversible, the damage rate is always a non-negative quantity. The damage model is briefly described in Appendix A and the details are reported by Ray et al. (1994) and Ray and Wu (1994).

The performance measure generator provides the damage controller with a measure of plant dynamic performance, P, which is a function of the reference trajectory, y^{ref}, as seen in Fig. 1. As an example, for the rocket engine under consideration in this paper, the measure of performance is chosen to be the average ramp rate of the reference trajectory for the main thrust chamber pressure from the beginning of the maneuver to the present time:

$$P(k) = f(y^{ref}(k), k) = \frac{y^{ref}(k) - y_i^{ref}}{kT - t_0} \tag{1}$$

where t_0 is the starting time of the transient; y_i^{ref} is the value of the reference trajectory at time $t = t_0$; k indicates the kth sampling instant; $y^{ref}(k)$ is the value of the reference trajectory at the kth sampling instant; and T is the sampling time of the A/D sampler and D/A zero order hold.

The reference signal generator takes the ramp rate specified by the damage controller and integrates it to obtain the reference signal. It is in the form of an integrator:

$$y^{ref}(k+1) = y^{ref}(k) + RR(k)T. \tag{2}$$

The purpose of the damage controller is to dynamically alter the ramp rate of the reference trajectory during the transient. The output of the damage controller is zero before and after the transient and is constrained to lie within a pre specified range, $RR_{min} \le RR(k) \le RR_{max}$, during the transient.

3 Sampled-Data Tracking Controller for a Rocket Engine

The synthesis of a damage mitigating control system is demonstrated for a reusable rocket engine following the control system architecture in Fig. 1. The sampled-data tracking controller in the inner loop is designed by using the H_∞ or induced L_2-norm technique which minimizes the worst case gain between the energy of the exogenous inputs and the energy of the regulated outputs. Bamieh and Pearson (1992) proposed a solution to the induced L_2-norm control synthesis problem for application to sampled-data systems. This design procedure has subsequently been incorporated as the function sdhfsyn in the MATLAB mutools toolbox (Balas, Doyle et al., 1993).

Figure 2 shows the setup used for the synthesis of the induced L_2-norm controller for the rocket engine based on a plant model with two inputs, fuel preburner oxidizer valve position and oxidizer preburner oxidizer valve position, and two outputs, main thrust chamber hot-gas pressure and O_2/H_2 mixture ratio. The plant model is obtained by first linearizing an 18 state nonlinear model of the rocket engine which does not contain actuator dynamics (Ray and Dai, 1995) at a combustion pressure of 17.58 MPa (2550 psi) and an O_2/H_2 ratio of 6.02. The pressure 17.58 MPa (2550 psi) is chosen for linearization because the controller is required to operate in the range 14.48 MPa (2100 psi) to 20.69 MPa (3000 psi). After linearization, the 18 state linear model is reduced to a 13 state linear model for the controller design via Hankel model order reduction (Zhou et al., 1996). A comparison of Bode plots reveals that the 13th order model does not significantly alter the input-output characteristics of the original 18th order model. However, the use of Hankel model order reduction may cause the resulting reduced model to have a non-zero D-matrix even if the original model is strictly proper. Since the induced L_2-norm controller synthesis requires a strictly proper generalized plant model, the problem of a non-zero D-matrix is circumvented by augmenting the reduced order model with actuator dynamics for each of the two inputs repre-

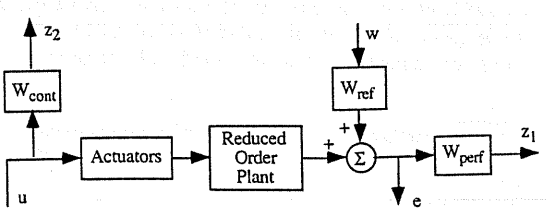

Fig. 2 Linear controller synthesis

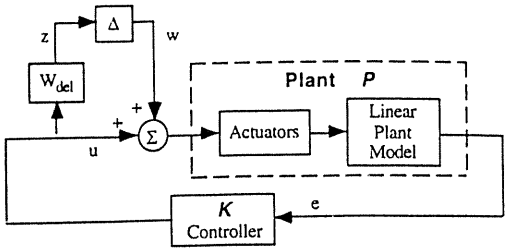

Fig. 3 Robust stability analysis

sented by a unity gain first order low pass filter (of time constant 3 ms). Therefore, the order of the reduced model with actuator dynamics is 15.

The frequency-dependent performance weight, W_{perf}, consists of two components: W_{press}, which penalizes the tracking error of combustion chamber pressure, and W_{O_2/H_2}, which penalizes the tracking error of O_2/H_2 ratio. The gain of the performance weights is related to the steady state error at low frequencies and to the transient part of the tracking error at high frequencies. The objectives of the performance weights in this application are to keep steady-state error and overshoot/undershoot small while, at the same time, allowing a reasonably fast rise time. The frequency-dependent control signal weight, W_{cont}, consists of two components: W_{H_2} which penalizes the fuel preburner oxidizer valve position, and W_{O_2} which penalizes the oxidizer preburner oxidizer valve position. The objectives of these control signal weights are: (*i*) prevention of large oscillations in the feedback control signal that may cause valve saturation; and (*ii*) reduction of valve wear and tear due to high-frequency movements.

The parameters of both performance weights and control signal weights are initially selected based on the control system performance requirements and the knowledge of plant dynamics; subsequently, the parameters are fine-tuned based on (frequency-domain) robust stability analysis and (time-domain) responses of the simulation experiments. In the present design, the performance weights are:

$$W_{press}(s) = 2\left(\frac{s + 0.75}{s + 3}\right);$$

$$W_{O_2/H_2}(s) = 1760\left(\frac{s + 0.045}{s + 0.8}\right) \tag{3}$$

and the control weights are chosen to be the same for both valves:

$$W_{H_2} = W_{O_2} = 4000\left(\frac{s + 10}{s + 100}\right) \times \frac{1 \times 10^5}{s + 1 \times 10^5} \tag{4}$$

where the additional high frequency dynamics in Eq. (4) ensure that the generalized plant model is strictly proper, which is necessary for reasons discussed earlier. Each of the two components of the frequency-dependent disturbance weight, W_{ref}, in Fig. 2 is chosen to be:

$$W_{ref}(s) = \frac{0.5}{s + 0.5}. \tag{5}$$

The rationale for selecting the above transfer function is that the bandwidth of the trajectory reference signals is expected to be less than 0.5 rad/s.

The input multiplicative configuration is chosen to represent the plant model uncertainties due to actuator errors and neglected high frequency dynamics. The sampler and zero order hold associated with the controller are implicit in the setup used for robust stability as shown in Fig. 3. Each of the two components of the frequency-dependent disturbance weight, W_{del}, in Fig. 3 is chosen to be

$$W_{del}(s) = \frac{s + 1}{s + 10}, \tag{6}$$

which implies that the amount of plant uncertainty is estimated as being approximately 10 percent at low frequencies and 100 percent at high frequencies. The uncertainty model is constructed based on the assumptions of the rocket engine design and operation (Ray and Dai, 1995) and can be updated as additional analytical or experimental data become available. Since the plant model is validated with steady-state design data, it is more accurate in the low frequency range. The 18th order plant model is a finite-dimensional lumped-parameter model which may not adequately represent the dynamics of high frequency modes. This leads to the presence of a larger amount of uncertainty in the high frequency region of the model as compared to the uncertainty at low frequencies. Robust stability is analyzed based on the original linearized model, i.e., the model before order reduction.

A sufficient condition for induced L_2-norm-based robust stability for sampled data systems is that the induced L_2-norm of the transfer matrix from w to z in Fig. 3 is less than unity (Sivashankar and Khargonekar, 1993). The design scheme shown in Fig. 2 does not explicitly include robust stability. However, robustness is in some sense related to the presence of the control signal weight W_{cont} in the controller design. To see this let the "actuators" and "linear plant model" in Fig. 3 be lumped together and be denoted as P and let the "actuators" and "reduced order plant" in Fig. 2 be lumped together and be denoted as P_{red}. Also, let the "controller" in Fig. 3 be denoted as K and assume that this same controller is connected between e and u in Fig. 2. Then the transfer function from w to z in Fig. 3 is

$$T_{z,w} = W_{del}(I - KP)^{-1}KP \tag{7}$$

and the transfer matrix from w to z_2 in Fig. 2 is

$$T_{z_2,w} = W_{cont}(I - KP_{red})^{-1}KW_{ref}. \tag{8}$$

Notice that W_{cont} and W_{del} are somewhat similar in the sense that they both penalize high frequency components more than low frequency components. Also, W_{ref} and P are similar in the sense that both are low pass in nature, and P_{red} and P have essentially the same dynamics. Therefore, making the transfer matrix from w to z_2 in Figure 2 small tends to make the transfer matrix from w to z in Fig. 3 small. If the setup in Fig. 2 produces a robust controller, then computationally intensive methods such as μ-synthesis (Packard and Doyle, 1993) are not necessary.

Using the generalized plant from Fig. 2, a sampled-data controller is designed which is optimal in the induced L_2-norm sense. As guaranteed by the design method employed, the controller has 23 states, which is the same as the number of states in the generalized plant model which consists of the reduced order plant model (13 states), actuators (2 states), performance weighting matrix (2 states), reference signal weighting matrix (2 states), and control signal weighting matrix (4 states). The controller provides acceptable reference signal tracking for the plant without using a large amount of control effort. The induced L_2-norm of the transfer matrix from w to z in Fig. 3 is evaluated to be 0.993 (<1.0). Hence, the closed-loop system in the inner loop is robustly stable for the chosen uncertainty description. Reducing the order of the sampled-data controller from 23 states to 14 states causes no significant change in the controller dynamics from an input/output point of view. There is no significant change in the simulation results and the robust stability measure is unchanged up to 3 decimal places. Therefore, the 14-state controller is used in what follows. Plots dis-

playing the tracking capabilities of the sampled-data controller are presented in Section 5.

4 Design of a Fuzzy Damage Controller for a Rocket Engine

The task of performance/damage tradeoff belongs to the class of approximate-reasoning-based decision-making which is in the realm of human intelligence. Therefore, we have adopted a fuzzy-logic-based approach for the damage controller design that can emulate the decision-making capabilities of a human operator (Pedrycz, 1992). In this section, we demonstrate how fuzzy-logic-based decisions can be used as a possible solution to the damage-mitigating control problem in rocket engines. It is cognitively intuitive that if an excessive damage rate or damage accumulation is detected during a ramp-up transient, reduction of the combustion chamber pressure ramp rate is likely to decrease the damage rate in turbine blades; this knowledge needs to be precisely quantified for fuzzy controller synthesis. Since it is difficult to acquire the actual experience of operating rocket engines, an intuitive knowledge base is generated from a variety of computer simulation experiments to identify the trends of the rocket engine. The standard components of a fuzzy controller (Pedrycz, 1992) are described below from the perspectives of damage mitigation in the blades of a rocket engine turbine.

4.1 Fuzzy Rule Base. The measure of performance is chosen in this application as the average ramp rate of the pressure reference signal from the starting time of the maneuver, t_0, to the current time, $t > t_0$. Three universes of discourse (X_j, $j = 1, 2, 3$) are defined for this application: one for damage rate, one for performance, and one for the ramp rate of the thrust chamber pressure reference trajectory. The three universes of discourse ($X_j, j = 1, 2, 3$) and the associated sets of membership functions are defined as follows:

Natural Logarithm of Damage Rate:
universe of discourse: $\dot{d} \in X_1 = (-\infty, \infty)$
membership functions: $\dot{\mathbf{D}} = \{\dot{D}_1, \dot{D}_2, \ldots, \dot{D}_{n_1}\}$
where $D_i: X_1 \rightarrow [0, 1], \quad i = 1, \ldots, n_1$

Performance:
universe of discourse: $p \in X_2 = [RR_{\min}, RR_{\max}]$
membership functions: $\mathbf{P} = \{P_1, P_2, \ldots, P_{n_2}\}$
where $P_i: X_2 \rightarrow [0, 1], \quad i = 1, \ldots, n_2$

Ramp Rate:
universe of discourse: $rr \in X_3 = [RR_{\min}, RR_{\max}]$

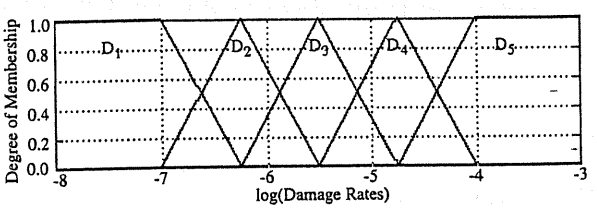

Fig. 4 Damage rate membership functions

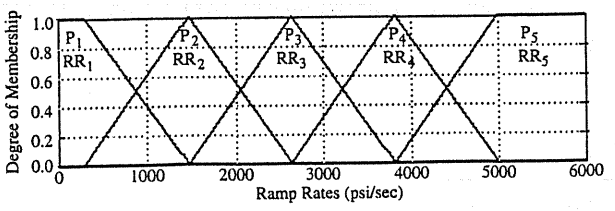

Fig. 5 Ramp rate and performance membership functions

Table 1 If-Then rules for fuzzy controller

	D_1	D_2	D_3	D_4	D_5
P_1	RR_5	RR_4	RR_3	RR_2	RR_1
P_2	RR_5	RR_4	RR_3	RR_2	RR_1
P_3	RR_5	RR_3	RR_2	RR_2	RR_1
P_4	RR_5	RR_3	RR_2	RR_1	RR_1
P_5	RR_5	RR_3	RR_1	RR_1	RR_1

membership functions: $\mathbf{RR} = \{RR_1, RR_2, \ldots, RR_{n_3}\}$
where $RR_i: X_3 \rightarrow [0, 1], \quad i = 1, \ldots, n_3$

The extreme points $RR_{\min}$ and $RR_{\max}$ are design variables which represent the minimum and maximum allowable ramp rates and the positive integers n_1, n_2, and n_3 are design variables representing the cardinalities of the membership function sets. The lower bound of the ramp rate is chosen to be $RR_{\min} = 300$ psi/s and the upper bound is chosen to be $RR_{\max} = 5000$ psi/s based on the operating procedure of the rocket engine (Ray and Dai [1995]). For the current design, $n_1 = 5$ with the $\dot{D}_i$'s representing:

- $\dot{D}_1$ = very low damage rate
- $\dot{D}_2$ = low damage rate
- $\dot{D}_3$ = moderate damage rate
- $\dot{D}_4$ = high damage rate
- $\dot{D}_5$ = very high damage rate

A plot of the five damage rate membership functions is shown in Fig. 4. Similarly, Fig. 5 shows the performance and ramp rate membership functions with $n_2 = 5$ and $n_3 = 5$. For this specific application, the performance, **P**, and ramp rate, **RR**, membership functions are made identical to each other for simplification of the control law without compromising the controller effectiveness. However, in general, **P** and **RR** may be different from each other. Furthermore, all membership functions are chosen to be triangle functions that cross each other at the membership value of 0.5. In general, any typical membership function shapes (e.g., Gaussian) can be used.

Once the membership functions are defined, they are combined into a set of $N = n_1 * n_2$ Fuzzy Control Rules:

Rule 1: If $\dot{D}^1$ and P^1 then RR^1

Rule 2: If $\dot{D}^2$ and P^2 then RR^2

$\vdots$

Rule N: If $\dot{D}^N$ and P^N then RR^N,

where $\dot{D}^i \in \dot{\mathbf{D}}$, $P^i \in \mathbf{P}$, and $RR^i \in \mathbf{RR}$. For example, the ith rule could be chosen as:

If $\dot{D}_5$ and P_3 then RR_1 which, with appropriate definitions of $\dot{D}^i = \dot{D}_5$, $P^i = P_3$, and $RR^i = RR_1$, represent:

If damage rate is very high and performance is moderate, then set the ramp rate to a very small value.

The experience of a human operator is captured and stored in the above rules. Table 1 lists a set of if-then rules for the fuzzy controller of the rocket engine under consideration. Note that, in this case, the first two rows of Table 1 are identical. Therefore, for this particular choice of if-then rules, it is possible to combine the first two rows into a single row without changing the input-output mapping of the fuzzy controller.

4.2 Fuzzy Inputs and Fuzzifier. The inputs to the Inference Mechanism of the fuzzy controller are fuzzy sets representing the current measure of damage rate and performance. There are two possible formats for the damage rate input to the fuzzy controller. If information about the current measure of damage is known in the form of a probability density function (pdf)

(Ray and Tangirala, 1997), then the fuzzy input mapping $\dot{D}$: $X_1 \rightarrow [0, 1]$ is simply this (pdf) where $\dot{D}(\dot{d})$ is large at those values of $\dot{d} \in X_1$ that are expected to be the true value of the current damage rate. If the damage input is a deterministic quantity, then a fuzzy singleton should be used:

$$\dot{D}(\dot{d}) = \begin{cases} 1 & \text{when } \dot{d} = E[\text{current damage rate}] \equiv \bar{\dot{d}} \\ 0 & \text{otherwise} \end{cases} \quad (9)$$

The simulation experiments in this paper are based on a deterministic damage model because the stochastic model parameters for the material (i.e., Nickel-based superalloys) are not available; the deterministic rule in Eq. (9) can be easily replaced by the damage pdf as it becomes available. Furthermore, since there are two damage rates, one each for the O_2 turbine and the H_2 turbine blades, $\bar{\dot{d}}$ is taken to be the maximum of the two damage rates. Since the performance measure is deterministic, a fuzzy singleton P: $X_2 \rightarrow [0, 1]$ is used as the fuzzy input:

$$P(p) = \begin{cases} 1 & \text{when } p \text{ equals the current performance measure} \equiv \bar{p} \\ 0 & \text{otherwise} \end{cases} \quad (10)$$

4.3 Inference Mechanism and Defuzzifier. The first phase of the decision process in the inference mechanism is the matching stage whose role is to determine the applicability of each fuzzy control rule to the present set of fuzzy inputs. To this end, the function $\lambda_i(\dot{D}, P)$ is defined for each of the N fuzzy control rules:

$$\lambda_i = \min \left\{ \max_{\dot{d} \in X_1} [\min (\dot{D}(\dot{d}), \dot{D}^i(\dot{d}))], \right.$$
$$\left. \max_{p \in X_2} [\min (P(p), P^i(p))] \right\}, \quad i = 1, \ldots, N. \quad (11)$$

Note that Eq. (11) is completely general in the sense that the fuzzy inputs, $\dot{D}$ and P, are not necessarily fuzzy singletons. If the two fuzzy inputs are in the form of fuzzy singletons, then Eq. (11) reduces to:

$$\lambda_i = \min \{ \dot{D}^i(\bar{\dot{d}}), P^i(\bar{p}) \}, \quad (12)$$

where $\bar{\dot{d}}$ and $\bar{p}$ are the current deterministic values of damage rate and performance. The λ_i's have a simple interpretation: $\lambda_i \in [0, 1]$ represents to what extent the current damage rate and performance inputs satisfy the "if" part (or antecedent) of the ith fuzzy control rule. If λ_i is large, then the ith rule should have a large role in determining the fuzzy controller output.

The second phase of the decision process in the inference mechanism is the summarizing stage whose role is to combine the λ_i's defined above with the RR^i's to produce a fuzzy controller output that is a deterministic quantity. A computationally efficient method to accomplish this task is presented below.

The first step is off-line identification of the centers of gravity, $\overline{rr}_i$, of each of the RR^i's. For the set of ramp rate membership functions chosen in Figure 5, if $RR^i = RR_j$, where $j = 2, \ldots, n_3 - 1$, then $\overline{rr}_i$ equals the $rr \in X_3$ for which $RR_j = 1$ (i.e., $RR_j(\overline{rr}_i) = 1$). If $RR^i = RR_1$, then $\overline{rr}_i = RR_{\min}$. If $RR^i = RR_{n_3}$, then $\overline{rr}_i = RR_{\max}$. The deterministic controller output is then chosen to be:

$$rr = \frac{\lambda_1 \overline{rr}_1 + \lambda_2 \overline{rr}_2 + \ldots + \lambda_N \overline{rr}_N}{\lambda_1 + \lambda_2 + \ldots + \lambda_N}. \quad (13)$$

In the summarizing stage, the controller output is created from a "linear combination" of all N fuzzy control rules. Note, however, that only the centers of gravity of the RR^i's are used but not their shapes.

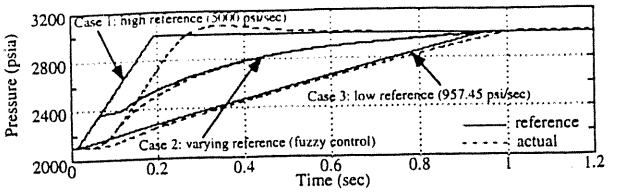

Fig. 6 Transients of thrust chamber pressure under all three cases

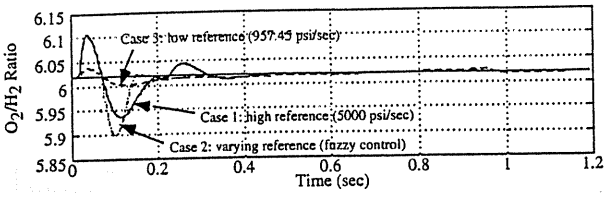

Fig. 7 Transients of O_2/H_2 ratio under all three cases

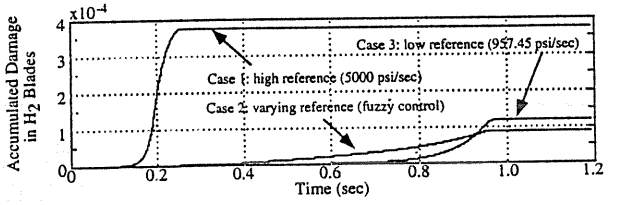

Fig. 8 Accumulated damage in H_2 blades under all three cases

4.4 Stability of the Damage Mitigating Control System. Stability of the closed-loop system is the single most important requirement of any controller design. While a necessary and sufficient condition for stability is easily obtained from the eigenvalues of the A-matrix in finite-dimensional linear time-invariant systems, there is no such straightforward condition for stability of nonlinear and/or time-varying systems. Since fatigue damage models induce severe nonlinearities, control systems containing a damage model in a feedback loop are nonlinear, and, in some cases, time-varying as well.

The inner control loop containing the discrete time tracking controller is a linear sampled-data system which has been shown to be robustly stable with respect to the uncertainty description shown in Fig. 3. To avoid the possibility of any signal in the two-tier control system in Fig. 1 becoming unbounded, the damage controller in the outer loop has been given limited authority in the sense that there are bounds on the ramp rates being generated by the fuzzy controller. In essence, the fuzzy controller does not have the ability to choose a chamber pressure reference signal which will cause the inner control loop to become unstable. However, this rate limit does not establish stability of the control system in the sense of Lyapunov. For example, there is no guarantee that phenomena like limit cycling of the reference signals will not occur. Analytical methods which may be successful in proving the stability and absence of limit cycles in damage-mitigating control systems include describing function and the absolute stability methods of Lur'e and Postnikov (Vidyasagar, 1992).

5 Results and Discussion

This section compares and discusses the results in Figs. 6 to 13 for three different simulation experiments of the reusable rocket engine under consideration. In each of the three cases the main thrust chamber pressure is increased from 14.48 MPa (2100 psi) to 20.69 MPa (3000 psi). Also, the O_2/H_2 ratio set point is set to a constant value of 6.02 for all cases following

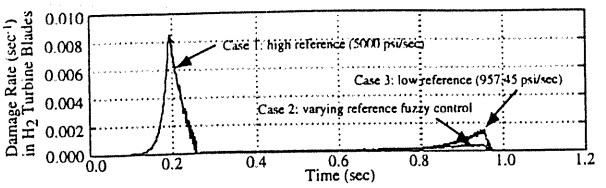

Fig. 9 Damage rate in H_2 blades under all three cases

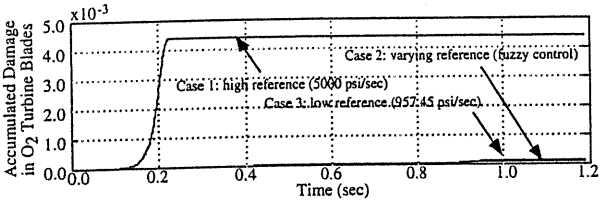

Fig. 10 Accumulated damage in O_2 blades under all three cases

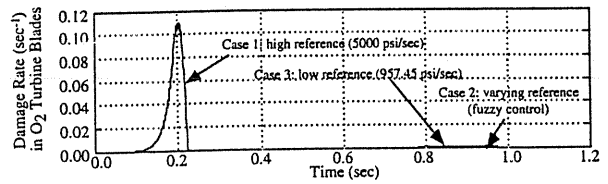

Fig. 11 Damage rate in O_2 blades under all three cases

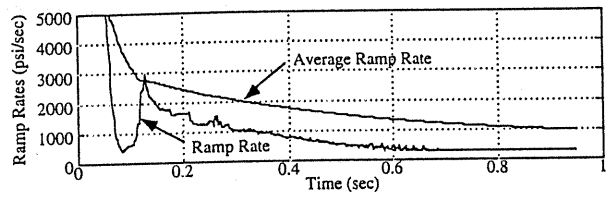

Fig. 12 Ramp rate and average ramp rate under fuzzy control (Case 2)

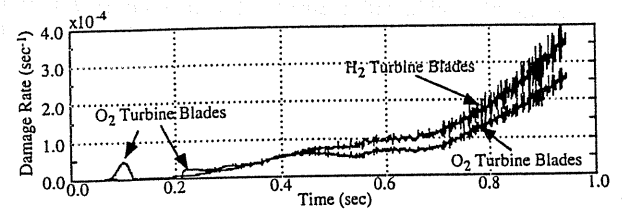

Fig. 13 Damage rates in O_2 and H_2 turbine blades under fuzzy control (Case 2)

the engine performance specifications (Ray and Dai, 1995). The three case are briefly described below:

Case 1 (High constant reference ramp rate): The rocket engine performance is specified in the terms of chamber pressure and O_2/H_2 ratio tracking errors without any penalty on damage rate and accumulation. Therefore, the reference signal is not a function of damage accumulation or damage rate. The reference pressure ramp rate is set to a constant value of 34.48 MPa/s (5000 psi/s) during the upthrust transients of the rocket engine. In order to follow the reference trajectory, the tracking controller attempts to maneuver the chamber pressure from its initial value to its final value as quickly as possible.

Case 2 (Varying reference ramp rate under fuzzy control): The fuzzy controller loop is activated in order to achieve a trade-off between performance and damage. The ramp rate of the pressure reference trajectory is allowed to change dynamically as a function of the current value of the damage rate in the O_2 and H_2 turbine blades as well as the current measure of performance following the procedure of Section 4.

Case 3 (Low constant reference ramp rate): This case is similar to Case 1 with the exception that the ramp rate is reduced to a constant value of 6.60 MPa/sec (957.45 psi/s). This is the average ramp rate based on the time interval of about 0.94 sec required for the pressure reference signal to reach 20.69 MPa (3000 psi) starting from 14.48 MPa (2100 psi) based on the results of the fuzzy controller simulation (Case 2).

Figure 6 shows that both the rise time and settling time are best for Case 1 and worst for Case 3. The 34.48 MPa/sec (5000 psi/sec) in Case 1 is the only one of the three cases that causes an overshoot in the pressure transients leading to a high damage rate. The pressure transients under fuzzy control in Case 2 are intermediate between the two extremes of fast and sluggish responses of Case 1 and Case 3, respectively. For all three cases the O_2/H_2 ratio in Fig. 7 is maintained within acceptable limits.

Figures 8 to 11 display the accumulated fatigue damage and damage rate of the H_2 and O_2 turbine blades for the three cases. For both blades, when the ramp rate is 34.48 MPa/s (5000 psi/s) in Case 1, the damage rate is extremely large for a brief period. This short burst of damage rate causes a relatively large accumulation of fatigue damage. The fatigue damage caused by the steep ramp rate in Case 1 is about 4.25 times more in the H_2 turbine blade and about 63.65 times more in the O_2 turbine blade than the respective damage for varying ramp rate under fuzzy control in Case 2. The damage accumulation in Case 3, with reduced ramp rate, is slightly higher than that in Case 2 although the pressure ramp rate is significantly more sluggish.

Figures 12 and 13 exhibit how the fuzzy controller operates. Since the damage rate in both blades is very small from the starting time of zero seconds to the instant of ~0.054 seconds, the fuzzy controller sets the pressure reference ramp rate to its maximum level of 34.48 MPa/s (5000 psi/s). At the instant of ~0.054 seconds the damage rate in the O_2 turbine blade begins to increase causing the fuzzy controller to abruptly decrease the reference ramp rate. This action prevents a large burst of damage rate that occurred in Case 1 under a constant ramp rate of 34.48 MPa/s (5000 psi/s). As the damage rate in the O_2 turbine blade begins to decrease at around 0.1 seconds, the fuzzy controller increases the ramp rate because of the following reasons: (*i*) the damage rate is decreasing; and (*ii*) the performance is now degraded as can be seen by the decrease in the average ramp rate plot in Fig. 12. Finally, as the pressure approaches its final value of 20.69 MPa (3000 psi), the damage rates of the two blades increase even though the fuzzy controller applies a small pressure ramp rate.

6 Summary and Conclusions

This paper presents a procedure for synthesis of a damage mitigating control system where the objective is to achieve a desired trade-off between performance and damage via feedback of on-line measurements of damage and damage rate. The proposed control system has a two-tier structure. A linear sampled-data controller tracks a reference trajectory vector in the lower tier while a fuzzy-logic-based damage controller at the upper tier makes a trade-off between system performance and damage in critical plant components. A formal proof of stability of the two-tier damage-mitigating control system is not presented in this paper; it is a topic of future research.

The synthesis procedure is demonstrated by simulation experiments on the model of a reusable rocket engine where the

fatigue crack damage in the turbine blades limits their service life. The performance variables of the rocket engine are expressed in terms of transients of main thrust chamber pressure and oxygen/hydrogen (O_2/H_2) mixture ratio. The results of simulation experiments for upthrust transients of the rocket engine operation show that the fuzzy controller is capable of regulating the performance/damage tradeoff in the turbine blades. The fuzzy controller chooses the reference signal for pressure ramp rate to be high at the beginning of the transients followed by a reduction of the ramp rate as the target pressure is approached. Since the fuzzy controller makes the decision of changing the pressure reference signal as a function of on-line damage prediction, it can react to unexpected situations, such as damage caused by external disturbances that cannot be predicted *a priori*. From the perspective of the trade-off between performance and damage, the simulation results indicate that dynamically maneuvering the ramp rate of the chamber pressure reference signal under fuzzy control is superior to the application of a constant ramp rate throughout the maneuver.

The concept of damage mitigating control is of significant importance to the operation of any plant where structural integrity is a critical issue. By including the on-line information of structural damage in the control scheme, not only is the service life of the controlled process extended, but also the mean time between major maintenance actions can be increased. For example, during a particular mission, if the damage rate in a plant component exceeds the expected level, it may be possible to modify the operation of the plant on-line so that the current mission can be completed with an acceptable amount of damage accumulation. The tradeoff could be a (possibly) small reduction in the plant performance. Changing the operation of the plant in this situation may also prevent a potentially catastrophic situation caused by the failure of a critical plant component. The implementation of damage mitigating control has the potential of providing both economic benefits and enhancement of operational safety.

Acknowledgments

The authors acknowledge benefits of discussion with Mr. Carl F. Lorenzo of NASA Lewis Research Center, and their colleagues at the Pennsylvania State University.

References

Balas, G. J., Doyle, J. C., et al., 1993, *μ-Analysis and Synthesis Toolbox*, MUSYN Inc., and The Math Works, Inc.

Bamieh, B. A., and Pearson, J. B., 1992, "A General Framework for Linear Periodic Systems with Applications to H_∞ Sampled-Data Control," *IEEE Transactions on Automatic Control*, Vol. 37, No. 4, Apr., pp. 418–435.

Bannantine, J. A., Comer, J. J., and Handrock, J. L., 1990, *Fundamentals of Metal Fatigue Analysis*, Prentice-Hall.

Dai, X. and Ray, A., 1996, "Damage-Mitigating Control of a Reusable Rocket Engine: Parts I and II," ASME JOURNAL OF DYNAMIC SYSTEMS, MEASUREMENT, AND CONTROL, Vol. 118, No. 3, Sept., pp. 401–415.

Dowling, N. E., 1983, "Fatigue Life Prediction for Complex Load Versus Time Histories," ASME *Journal of Engineering Materials and Technology*, Vol. 105, pp. 206–214.

Holmes, M. S., Tangirala, S., and Ray, A., 1997, "Life-Extending Control of a Reusable Rocket Engine," *American Control Conference*, Albuquerque, NM, June.

Paris, P. C., and Erdogan, F., 1963, "A Critical Analysis of Crack Propagation Laws," ASME *Journal of Basic Engineering*, Vol. 85, pp. 528–534.

Packard, A., and Doyle, J. C., 1993, "The Complex Structured Singular Value," *Automatica*, Vol. 29, pp. 71–109.

Pedrycz, W., 1992, *Fuzzy Control and Fuzzy Systems*, 2nd Ed., Wiley, New York.

Ray, A. and Wu, M-K., 1994, *Damage-Mitigating Control of Space Propulsion Systems for High Performance and Extended Life*, NASA Contractor Report 19440 under Lewis Research Center Grant NAG 3-1240.

Ray, A., Wu, M-K., Carpino, M., and Lorenzo, C. F., 1994, "Damage-Mitigating Control of Mechanical Systems: Parts I and II," ASME JOURNAL OF DYNAMIC SYSTEMS, MEASUREMENT, AND CONTROL, Vol. 116, No. 3, Sept., pp. 437–455.

Ray, A., and Dai, X., 1995, *Damage-Mitigating Control of a Reusable Rocket Engine*, NASA Contractor Report 4640 under Lewis Research Center Grant NAG 3-1240.

Ray, A., and Tangirala, S., 1997, "A Nonlinear Stochastic Model of Fatigue Crack Dynamics," *Probabilistic Engineering Mechanics*, Vol. 12, No. 3, pp. 33–40.

Sivashankar, N., and Khargonekar, P. P., 1993, "Robust Stability and Performance Analysis of Sampled-Data Systems," *IEEE Transactions on Automatic Control*, Vol. 38, No. 1, Jan., pp. 58–69.

Suresh, S., 1991, *Fatigue of Materials*, Cambridge University Press, Cambridge, UK.

Swain, M. H., Everett, R. A., Newman, J. C., Jr., and Phillips, E. P., 1990, "The Growth of Short Cracks in 4340 Steel and Aluminum-Lithium 2090," AGARD Report, No. 767, pp. 7.1–7.30.

Tangirala, S., Holmes, M., Ray, A., and Carpino, M., 1997, "Life-Extending Control of Mechanical Structures: Experimental Verification of the Concept," to appear in *Automatica*.

Vidyasagar, M., 1992, *Nonlinear Systems Analysis*, 2nd ed., Prentice-Hall, Englewood Cliffs, NJ.

Zhou, K., Doyle, J. C., and Glover, K., 1996, *Robust and Optimal Control*, Prentice-Hall, Upper Saddle River, NJ.

APPENDIX A

Models of the Rocket Engine Dynamics, Turbine Blade Structure, and Fatigue Damage

The reusable rocket engine under consideration is similar to the Space Shuttle main engine (Ray and Dai, 1995). The propellants, namely, liquid hydrogen fuel and liquid oxygen, are individually pressurized by separate closed cycle turbopumps. Pressurized cryogenic fuel and oxygen are pumped into two high-pressure preburners which feed the respective turbines with fuel-rich hot gas. The fuel and oxidizer turbopump speeds and hence the propellant flow into the main thrust are controlled by the respective preburner. The exhaust from each turbine is injected into the main combustion chamber where it burns with the oxidizer to make the most efficient use of the energy. The oxygen flow into each of the two preburners are independently controlled by the respective servo-valves while the valve position for oxygen flow into the main thrust chamber is held in a fixed position to derive the maximum possible power from the engine. The plant outputs of interest are oxygen/hydrogen (O_2/H_2) mixture ratio and main thrust chamber pressure which are closely related to the rocket engine performance in terms of specific impulse, thrust-to-weight ratio, and combustion temperature.

Plant Dynamic Model: A finite-dimensional state-space model of the rocket engine has been formulated via lumped parameter approximation of the partial differential equations describing mass, momentum, and energy conservation. The plant model is constructed by causal interconnection of the primary subsystem models such as main thrust chamber, preburners, turbopumps, valves, fuel and oxidizer supply header, and fixed nozzle regeneration cooling. The plant dynamic model consists of twenty state variables, two control inputs, and two measured variables (Ray and Dai, 1995).

Structural Model of Turbine Blades: The structural model in each of the fuel and oxidizer turbines calculates the cyclic mechanical stresses at the root of a typical blade which is presumed to be a critical point in this study. The blade model for each of the two turbines is represented by a three-node beam model with six degrees of freedom at each node while the first node at the root is fixed. The load on each blade model is assumed to consist of two components (Ray and Wu, 1994). The first component is due to the (time-dependent) drive torque which is derived as an output of the plant dynamic model. The second component is a dynamic term which represents the oscillatory load on the blade as it passes each stator. It is the second component that causes high cycle fatigue at the root of the blade while the first component is largely responsible for the mean stress. Since both the fatigue damage and subsequent crack initiation sites are confined within a small region of the blade, a linear elastic approach is adopted for macroscopic modeling of the structural dynamics and to predict transient stresses at the point of potential failure. In this approach, the blade

geometry, properties of the blade material, and plant state variables are used as inputs to a linear finite-element analysis program to generate a discretized representation of the blade structure and its loading conditions. The resulting stiffness matrix, mass matrix, and force vector are used to obtain a modal solution for the displacements. In the last step, the stress-displacement relations from the finite element analysis are used to predict the stresses at the critical point(s) of the blade structure.

Fatigue Damage Model of Turbine Blades: The fatigue damage model is first derived for linear damage accumulation following the Palmgren-Miner's rule and then modified following the damage curve approach to account for dependence of the damage rate on the current level of accumulated damage (Ray et al., 1994). Converting the strain amplitudes into stress amplitudes from the cyclic stress-strain curve, the rates of both elastic damage δ_e and plastic damage δ_p are computed through differentiation as:

$$\frac{d\delta_e}{dt} = 2\frac{d}{d\sigma}\left(\left(\frac{\sigma - \sigma_r}{2(\sigma_f' - \sigma_m)}\right)^{-(1/b)}\right) \times \frac{d\sigma}{dt} \times U(\sigma - \sigma_r) \quad \text{(A.1}a\text{)}$$

$$\frac{d\delta_p}{dt} = 2\frac{d}{d\sigma}\left(\frac{1}{\epsilon_f'}\left(\frac{\sigma - \sigma_r}{2K'}\right)^{1/n'}\left(1 - \frac{\sigma_m}{\sigma_f'}\right)^{-(c/b)}\right)^{-1/c} \times \frac{d\sigma}{dt} \times U(\sigma - \sigma_r) \quad \text{(A.1}b\text{)}$$

$$U(\theta) = \begin{cases} 1 & \text{for} \quad \theta \geq 0 \\ 0 & \text{for} \quad \theta \geq 0 \end{cases} \quad \text{(A.1}c\text{)}$$

where the current stress σ and the stress rate $d\sigma/dt$ are obtained from the structural model; σ_r is the reference stress obtained using the rainflow method (Dowling, 1983) $\sigma_m = (\sigma + \sigma_r)/2$ is the mean stress; and σ_f', ϵ_f', b, c, K', and n' are material parameters (Bannantine et al., 1990) under cyclic operations. The damage rate $d\delta/dt$ is obtained as the weighted average of the elastic and plastic damage rates such that

$$\frac{d\delta}{dt} = w\frac{d\delta_e}{dt} + (1 - w)\frac{d\delta_p}{dt} \quad \text{(A.2)}$$

where the weighting function, w, is selected as the ratio of the elastic strain amplitude and total strain amplitude. Equations (A.1) and (A.2) are then used to obtain the damage rate at any instant. Since the turbine blades are subjected to loads of varying amplitude, Eq. (A.1) which is based on the linear rule of damage accumulation will lead to erroneous results due to the sequence effect (Suresh, 1991). Therefore, the linear damage is modified via a nonlinear damage rule as follows:

$$D = (\delta)^{\gamma(\sigma_a, D)} \quad \text{(A.3)}$$

where D and δ are the current states of nonlinear and linear damage accumulation, respectively, and σ_a is the stress amplitude. It follows from a crack propagation model such as the Paris model (Paris and Erdogan, 1963) that the crack growth rate is dependent not only on the stress amplitude but also on the current crack length. Since the characteristics of γ in Eq. (A.3) may strongly depend on the type of the material, availability of pertinent experimental data for the correct material is essential for damage-mitigating control. An approach to evaluate γ at selected discrete levels of stress amplitude by interpolation based on the experimental data of Swain et al. (1990) is given by Ray et al. (1994).